Available online www.jsaer.com

***Journal of Scientific and Engineering Research*, 2018, 5(3):479-490**

Research Article

ISSN: 2394-2630
CODEN(USA): JSERBR

Effects of Heat Flux and Surface Roughness on the Pool Boiling of a Refrigerant, R134a

K. M. K. Pasha

Associate Professor of Mechanical Power, Faculty of Engineering, Modern University, Cairo, Egypt

Abstract The present work is devoted to investigate the heat transfer from a hot rough surface in a pool boiling of R134a surfactant solution. The surface roughness ranged from 0.5 to 22.5 μm, and the heat flux ranged from about 51 to 134 $kW.m^{-2}$. The saturation pressure was about 17 bars. The investigated cases are within the nucleate boiling stage of a pool boiling process. This investigation is executed using a controllable apparatus to minimize the need to human efforts, and to help save excess time and effort in the preparation of future investigations for new different cases. Digital and PID control techniques were used to control the operating conditions of the apparatus. The experiments showed that, the heat transfer coefficient increased with the heat flux, for all values of surface roughness. For the same heat flux, the heat transfer coefficient increased with the surface roughness. The percentage of increase in the heat transfer coefficient, at maximum heat flux, over that at minimum heat flux occurred with surface roughness of 1.4 μm, and was about 47%. An empirical correlation could be deduced from the experimental results. This correlation expressed the variation of the heat transfer coefficient as a function of the surface roughness, heat flux and the superheat temperature difference.

Keywords Boiling; Heat; Roughness; R134a.

Alphabetic

A	Plate area, πd2 / 4,	m^2,
d	Test plate diameter,	m
h	Heat transfer coefficient,	$W.m^{-2}.K^{-1}$
I	Electric current	Amper
N	number of thermocouples	
p	Pressure,	Pascal
Q	Total rate of heat transfer,	W
q	Heat per unit area of the test plate surface,	$W.m^{-2}$
Ra	average roughness height,	μm
T	Temperature	K
V	Electric potency	Volts

Subscripts

av	Average.
i	Thermocouple index
r	Refrigerant
s	Test plate surface

Greek symbols

ΔT Superheat temperature,	K.

Abbreviations

LCD Liquid-crystal display
PID Proportional, Integral, and Differential

1. Introduction

The pool boiling process is encountered in many engineering applications, and the most familiar of these, are the refrigeration systems. In such systems, the refrigerant passes in the evaporator tubes, whose surface temperatures are higher than the boiling temperature, that corresponds to its saturation pressure. Many researchers investigated the factors affecting the heat transfer during the pool boiling process with different types of refrigerants, in order to achieve a higher heat transfer coefficient. The work of these researchers, which is relevant to the present work will be discussed in brief.

1.1. Brief Survey of Previous Work

[1], compared the performance of R1234ze(E), the isomer R1234ze(Z), and R1233zd(E). The free convective condensation and pool boiling heat transfer coefficients (HTCs) of these refrigerants on a horizontal smooth tube made of copper with an outer diameter of 19.12 mm is comparatively assessed. They observed that, the role of surface tension on nucleate boiling was identified by the bubble behavior. [2], determined experimentally both spray evaporation and pool boiling heat transfer coefficients, using ammonia and titanium plain tubes. They concluded that, at the high heat flux range, spray evaporation heat transfer coefficients decrease with decreasing film flow rates, and the spray evaporation is particularly beneficial at the lower heat flux. They reported a heat transfer coefficient deterioration caused by dry patches. [3], used Ammonia as refrigerant which flows in tubes with enhanced surfaces in the evaporator.

That is to reduced the size and refrigerant charge of the evaporator by improving the heat transfer performance. They used commercial integral-fin (32 f.p.i., 1260 f.p.m.) titanium tube. They achieved average enhancement factor of 1.3. [4], studied the influence of sub-atmospheric pressure on nucleate boiling, in the pressure range 1–10 kPa and for heat flux densities 10–45 kW.m-2. Superheats were set between 6.2 and 28.7 K. They obtained experimentally values of heat transfer coefficients between1 and 2kW.m^{-2}K. The most accurate approximation of heat transfer coefficient was obtained using a reduced pressure correlation, and was within the range of (0.13–0.35). [5], investigated the pool boiling heat transfer performance of a low finned U-tube immersed in TiO /R141b nanofluid with four different nanoparticle loadings (0, 0.0001, 0.001, and 0.01 vol.%). An ultrasonic vibration crusher was used to inhibit the formation of the TiO_2 nano-sorption layer on the U-tube surface. The nano-fluid with a particle loading of 0.0001 vol. % yielded the optimal heat transfer performance, with a heat transfer coefficient around 30% higher than that of pure R141b refrigerant. [6], performed measurements of heat transfer coefficient obtained during flow boiling of R32 inside a brazed plate heat exchanger (BPHE). They investigated the effect of refrigerant heat flux, mass velocity, inlet vapor quality and superheating at the outlet, and a saturation temperature of 5 °C. They reported that, mass flux a high contribution of the convective term on the heat transfer coefficient. [7], experimentally investigated the heat transfer performance of R-134a and the effect of tube pitch on highly enhanced surface tube bundles. They studied three pitch-to-diameter ratios, (P/D), of 1.167, 1.33, and 1.5; all with a staggered triangle arrangement. They investigated two input variables: heat flux (5–60 kW.m^{-2}) and mass flux (15–55 kg/m^2.s). They concluded that, the smallest bundle showed a considerably lower performance than the other two, and the P/D 1.5 bundle uses more refrigerant compared to the P/D 1.33, which proves to be the optimum. [8], investigated the performance of a vapor injection refrigeration system using a mixture refrigerant R290/R600a, through steady-state simulations. They aimed to study the influence of the refrigerant composition on the following parameters: COP, compressor power, refrigerant mass flow rate, refrigerant temperature, mass flow ratio between vapor and feed streams in the flash tank liquid, vapor composition of flash tank outlet streams and compression ratio. A maximum COP was obtained for a mixture containing 40 wt% of R290, and the COP of vapor injection refrigeration cycle was 16–32% greater than that of a vapor compression cycle. [9], modeled the saturated flow boiling heat transfer characteristics of R134a flowing through micro- and macro-tubes. Ranges of the database cover mass fluxes between 50.0 and 1500.0 kg/m^{-2}.s^{-1}, heat fluxes between 3.0 and 150.0 kW.m^2, hydraulic diameter between 0.5 and 13.84 mm, saturation temperatures between −8.8 and 52.4 ◦C, and vapor qualities up

to 1.0. Their results indicated that, their new method, which has a mean absolute deviation of 19.1% and captures 66.7 and 83.2% of the experimental data within ±20 and ±30% error bands correspondingly, outperforms the available flow boiling correlations in the literature in terms of prediction accuracy. [10], performed a set of experiments to quantify the pool boiling heat transfer coefficient of water/γ-alumina micro-fluids at mass concentration ranged from 0.1 to 0.4 % of micro-particles with mean size of 1–2 μm. Influence of heat flux, mass concentration of micro-particles and surface fouling resistance on the pool boiling heat transfer coefficient were investigated. They showed that, micro-fluids have relatively higher thermal conductivity rather than the base fluids, and reported a significant deterioration of heat transfer coefficient of micro-fluids in comparison with the base fluid over the extended time (1000 min of operation) in nucleate boiling region. [11], investigated the boiling heat transfer and pressure drop of hydrocarbon refrigerant (R600a), which flow in six minichannels with fillisters. These fillisters are made by electrical-discharge machining, at inlet pressure of 259–293 kPa, and under saturated conditions. The mass flux was within the range of 195–487 $kg.m^{-2}.s^{-1}$ and heat flux of 1,790–8,950 $W.m^{-2}$. Their results of the mini-channels with fillisters (Tests 1–4) showed that the heat transfer coefficients increase about 1.05–1.34, 1.11–1.25, 1.23–1.59 and 1.07–1.21- fold, respectively. [12], performed experimental investigation of boiling heat transfer of refrigerant R-21 in upward flow over a vertical plate-fin heat exchanger with transverse size of the channels that is smaller than the capillary constant. They investigated the heat transfer coefficient in small values of mass velocities and heat fluxes. Their results showed a weak dependence of heat transfer coefficient on equilibrium vapor quality, mass flow rate, and heat flux density and do not correspond to calculations by the known heat transfer models. [13], injected SO_2 gas into different pure liquids via meshed tubes, to investigate the pool boiling heat transfer coefficient of pure liquids around the horizontal cylinder at different heat fluxes up to 114 kW m^{-2}. Their results demonstrate that presence of SO_2 gas into the vapor inside the bubbles creates a mass transfer driving force between the vapor phase inside the formed bubbles and liquid phase and also between the gas/liquid interfaces. The injection process increased the turbulence intensity in the convected fluid, and lead the pool boiling heat transfer coefficient to be dramatically enhanced. [14], investigated the heat transfer coefficient in a nucleate pool boiling process. He used R-134a, as a refrigerant, which is heated by different hot rough surfaces, with different heat fluxes. He concluded that, the heat transfer increased with the heat flux, for all values of surface roughness, and the normalized heat transfer coefficient increased with the normalized pressure for all values of heat flux. [15], experimentally investigated the roughness effects on nucleate pool boiling of refrigerant R113 on horizontal circular copper surfaces. The copper samples were treated to have different roughness values of 0.901, 0.735, 0.65, and 0.09, respectively, and the used heat flux within a range of 8 to 200 $kW.m^{-2}$. They concluded that, at heat flux of 170 $kW.m^{-2}$, the heat transfer coefficient of the sample with Ra=0.901 is 3.4, 10.5, and 38.5% higher than those of the surfaces with Ra of 0.735, 0.65, and 0.09, respectively. [16] modified the characteristics of a sandblasted surface of a cylindrical copper block, and applied a high intensity electrostatic field, in a saturated pool boiling of R-123 at 1 bar, including the critical heat flux (CHF). They achieved a considerable increase in the heat transfer rates, and accordingly the heat transfer coefficient. [17], determined experimentally the effects of the surface roughness of copper, brass and stainless steel on nucleate boiling heat transfer of refrigerants R-134a and R-123.

They reported significant effects of the surface material, with brass being the best performing and stainless steel the worst. [18], investigated the saturated pool boiling of halocarbon refrigerants on copper, brass and stainless steel surfaces, with different finishing conditions. They concluded that, for all surface materials, the heat transfer coefficient increased with surface roughness. [19], investigated the flow boiling heat transfer with the refrigerants R-134a and R-245fa in copper micro-channel cold plate evaporators. They used arrays of micro-channels with a rectangular cross section of hydraulic diameters 1.09 mm and 0.54 mm. The aspect ratio was 2.5. They reported that, the heat transfer coefficient is found to vary significantly with heat flux and vapor quality, but only slightly with saturation pressure and mass flux, and the nucleate boiling dominates the heat Transfer. They also assessed several flow boiling heat transfer Correlations for applicability to their experiments.

1.2. Objectives of the Present Work

In the present work, a controllable test rig is implemented to investigate the effect of the heat flux and surface roughness on the heat transfer coefficient, in a nucleate pool boiling. Table 1 illustrates the different studied cases.

Table 1: The Investigated Cases

No.	Roughness, Ra, µm	Heat flux, kW.m^{-2}	No.	Roughness, Ra, µm	Heat flux, kW.m^{-2}	No.	Roughness, Ra, µm	Heat flux, kW.m^{-2}	No.	Roughness, Ra, µm	Heat flux, kW.m^{-2}
1	0.5	134	5	1.4	134	9	2.8	134	13	22.5	134
2	0.5	106	6	1.4	106	10	2.8	106	14	22.5	106
3	0.5	76	7	1.4	76	11	2.8	76	15	22.5	76
4	0.5	51	8	1.4	51	12	2.8	51	16	22.5	51

2. Experimental Preparations

2.1. The Test Rig

The test rig, figure 1, consists mainly of an insulated room to control the temperature around the evaporator, which is located in the center of the room. This evaporator is full of the refrigerant and contains the hot test plate, where, the pool boiling occurs. The following subsections describe the different apparatus components.

2.1.1. The Insulated Room

A carbon-steel L-beam, whose dimensions are 8 x 8 x 0.8 cm, from which the outer frame of the insulated room is built. The room has dimensions 100 x 100 x 180 cm and is shielded by 8 cm asbestos layer, which is fixed between two galvanized steel sheets. Two glass windows, one is on the left side of the room, and the other is on the right side. Another two glass windows, one on each of the right and left sides of the evaporator, and have the same centerline as the room windows. So, on each of the right and left sides, there is a window in the room wall, which faces another window in the evaporator. These windows are used to monitor the boiling process on the hot test plate inside the evaporator. To control the temperature inside the insulated room, there is a heat exchanger, which receives water from the water supply unit at a controlled rate and temperature, in order to adjust the room temperature if changed. A variable speed air fan is placed in the bottom of the room to ensure a homogeneous temperature everywhere in the room

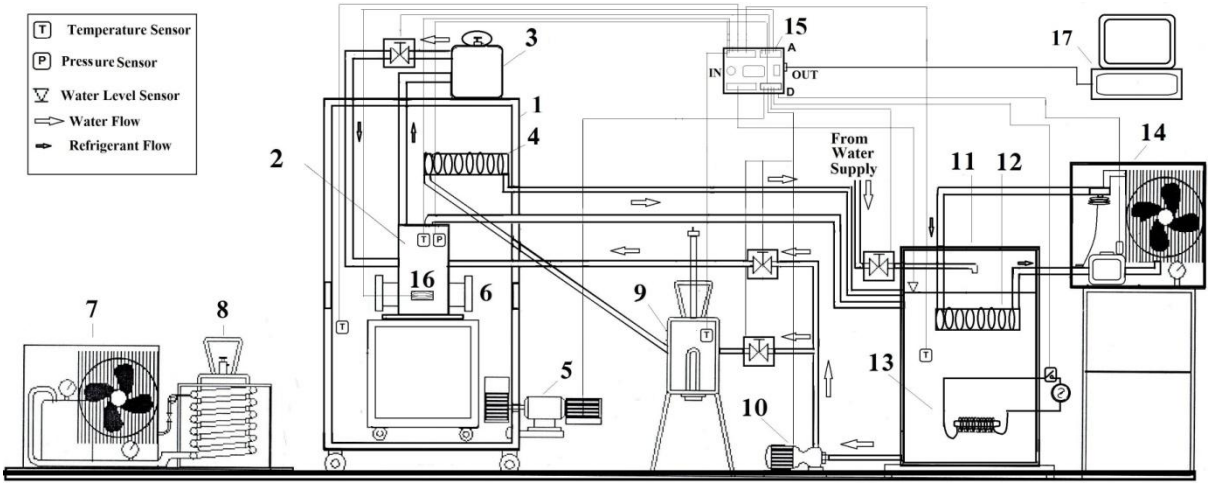

Figure 1: Test Rig

1-Insulated Room 2-pressure vessel 3-refrigerant tank
4-heat exchanger, (for hot water) 5-motor and fan 6-monitoring windows
7-refrigeration unit (collection) 8- evacuated vessel 9- heating tank

10-motor and pump 11- the water tank
12-heatexchanger,(refrigerant) 13-electric heater
14-refrigeration unit, (for tank) 15-the controller
16-the heating coil 17-The computer

2.1.2. The Evaporator, (Pressure Vessel)

It is a steel cylinder, figure 2, whose inner diameter and height are 250 and 390 mm, respectively, and its wall thickness is 20 mm. inside the evaporator, there is a heat exchanger, which receives the cold water from the water supply unit to condense the refrigerant vapor again after the boiling process. The test plate is located on the top of a heating element, which consists of a nickel chromium coil that is wound around an electric insulator. This heater is placed in a copper cylindrical cover, whose side and bottom walls are thermally insulated.

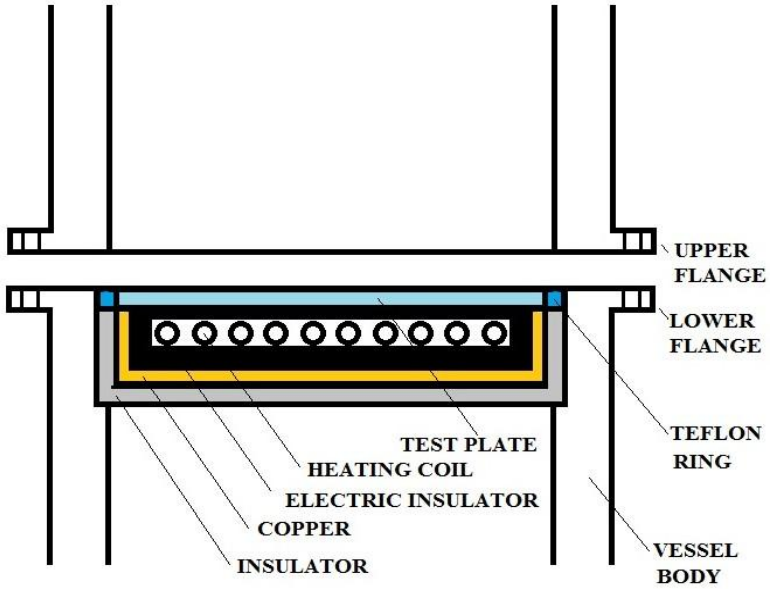

Figure 2: The Pressure Vessel

2.1.3. The Water Supply Unit

The water supply unit consists of the following;

1) The water tank whose capacity is one cubic meter, is insulated by a glass wood.
2) An electric heater, that increases the water temperature when it decreases below the required temperature.
3) A heat exchanger that consists of a coiled tube immersed in the water and circulates refrigerant supplied from a simple refrigeration system, in order to decrease the water temperature when it increases over the required temperature.
4) Since the warm water required to maintain the Insulated Room is supplied from the same water tank, then it is necessary to heat it in a separate heating tank, which is connected to the water tank through a piping system and solenoid bypass valves
5) A pump circulates the water to the two heat exchangers, inside the insulated room and the evaporator.
6) A controlled valves that open \ close to pass the cold \ warm water to any of the heat exchangers in the insulated Room or the pressure vessel.

2.1.4. The Hot Test Plates

It is a circular steel plate whose diameter and thickness are 192 and 3 mm, respectively, and is thermally isolated with a Teflon ring, that surrounds it. An electrical discharge machine (EDM), is used to produce five plates with different average roughness height.

2.1.5. The Refrigerant Collecting Unit

Consists of a separate simple refrigeration system, whose evaporator is a coil surrounds an evacuated vessel to cool it and decreases its pressure. When the pressure vessel is connected to the evacuated vessel, the refrigerant transfers to the evacuated vessel.

2.1.6. Measuring and Safety Devices

To measure the average surface temperature of the test plate surface, four thermocouples are distributed on a circular path on the test plate surface, and are equally spaced from each other, and this circular path has a radius of 80 mm. There are another eight thermocouples to measure the refrigerant temperature near the test plate surface. One thermocouple is in the saturated liquid refrigerant temperature, that fills the evaporator, in order to monitor the stability of the saturation condition and one thermocouple is in the insulated room to check the temperature around the vessel. All these thermocouples are of type, Copper-constantan, and are connected to the controller through number of MAX31855K interfaces. A high pressure sensor is secured inside the evaporator to monitor the required saturation pressure for the refrigerant. If the insulated room temperature increased, the controller sends digital signals to the solenoid bypass valves, which allows the cooling water to circulate in the heat exchanger, and to decrease the insulated room temperature.

Also if the insulated room temperature decreased, the controller sends digital signals to the solenoid bypass valves, to allow the hot water to circulate instead. In both cases, the controller sends a signal to the fan inside the insulated room to help mix the air and to ensure uniform room temperature.

2.2. The Experimental Procedure

Before starting the experimental work, it is essential to check the whole apparatus. The water is allowed to circulate in its passages and is monitored for 15 minutes to check if any leakage exists. The control sensors are calibrated by previously known values of temperature and pressure using a simulating software. To ensure no leakage

in the two refrigeration systems of the water supply unit and the refrigerant collecting unit, they were filled with N2 at a pressure of 5 bar to 7 bar and this pressure is maintained and monitored for 45 minutes. The evaporator is first, checked for no leakage by filling it with pressurize water, and after that, it is cleaned by liquid acetone, and dried by hot air. After this general check, the following procedure is executed in every experiment;

1) The required test plate is horizontally fixed on the top of the heating element using the Teflon ring, and the heating element is fixed in the lower threaded flange
2) After checking the Teflon ring position between the lower and the upper flanges, they are fixed to each other.
3) The evaporator is evacuated using a compressor.
4) The refrigerant tank, located over the insulated room, is allowed to fill the evaporator by about 8 kg of R134 refrigerant.
5) The controller opens\closes the bypass valves to feed the evaporator heat exchanger with hot water in the evaporator, until the refrigerant temperature and pressure are 61 ^{o}C and 17 bars, respectively, (saturated liquid).
6) The power supplied to the heating element, and consequently, the required heat flux, is fed to the controlling program through a touch screen.
7) When all the thermocouples approach their steady state readings, with fluctuations within the range of $\pm$ 1%, the controller starts the heating element, which will heat the test plate.
8) When the refrigerant, which is adjacent to the test plate, starts to evaporate, and the pressure changes, the controller circulates cold water to the evaporator exchanger to condense the refrigerant and retrieve the saturation pressure again.
9) During the experiment, the controller opens \ closes the bypass valves of the water supply unit to keep the insulated room temperature equal to the saturation temperature inside the evaporator.

10) Since the conductive heat losses, through the side and bottom walls of the insulated heating element, were estimated, in the worst case, to be about 1.7 % of the total electrical power, so; the control program calculates the heat flux and heat transfer using the simple equations;

$$Q = (98.3 / 100) \times (V) \times (I) \quad (1)$$

$$q = Q / A_s \quad (2)$$

$$T_{s,av} = \sum T_{si} / N \quad (3)$$

$$T_{r,av} = \sum T_{si} / N \quad (4)$$

$$h = (Q) / [A_s (T_{s,av} - T_{r,av})] \quad (5)$$

These calculated values of the heat flux and heat transfer coefficient appear on the LCD, and after they oscillate about fixed values, they are recorded. An error analysis is illustrated in appendix (A).

2.4. Data Validation

For the purpose of validation, the results of the present experimental work, for the heat transfer coefficient, were compared to the previous work. Figure 3 illustrates a comparison of the present work for cases; 9, 10, 11, and 12 with the work of [14]. The results of the present work, slightly exceeds those of [14], that is because, the present experiments were executed with a pressure of about 17.1 bar, whereas, the used pressure in [14] was about 16.5, and, it is proven that, the pressure factor considerably, affects the pool boiling heat transfer coefficient, [5]. Also, in the present work, the side and lower walls of the heating element were carefully isolated, which helps decrease the heat losses, and accordingly decrease the temperature differences, which results in a higher heat transfer coefficient for the same heat flux. Figure 4 illustrates another comparison of the present work for cases; 1, 2, 3, and 4 with the work of [15] and [19]. The results of Hosseini is lower than those of the present work, because, he executed his experiments with refrigerant R113. It was observed that, when decreasing the carbon and fluorine atoms in the molecular structure results in a decrease in its thermal properties, which in turn, results in a lower thermal performance. These lower thermal activities are most probable to reduce the heat transfer coefficient. The effect of decreasing the refrigerant thermal activities is more obvious with the lower heat flux, where, a lower heat flux passes to the surrounding liquid molecules, and results in, larger temperature difference and consequently, a lower heat transfer coefficient. In the compared case of [19], it is obvious that, the heat transfer has higher values than those of [15], this may be because, the microchannels increased the area through which, the heat transfer occurs, and they also behaved as a roughness, which promotes for the turbulent mixing. So, using the microchannels increases the heat transfer coefficient.

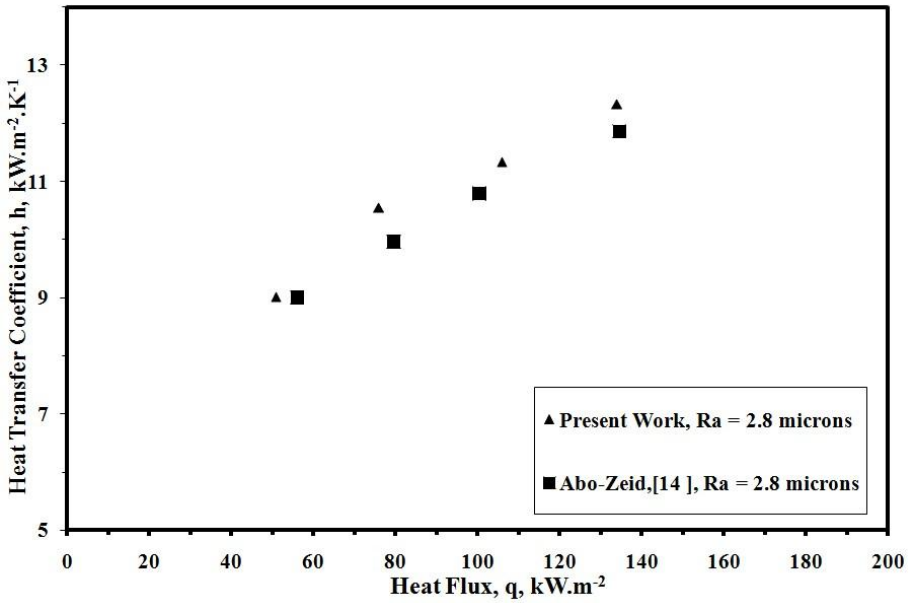

Figure 3: Comparison of the present work with [14]

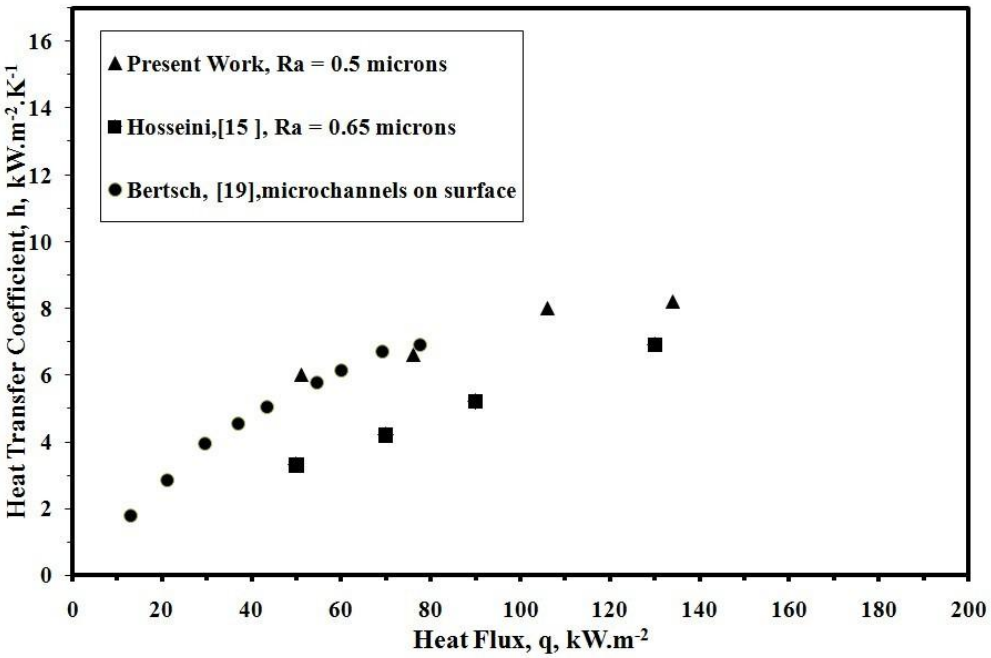

Figure 4: Comparison of the present work with [15] and [19].

3. Results and Discussion

In the present work, the pool boiling process was investigated over four heated plates with different surface roughness, which is within the range from 0.5 μm to 22.5 μm. Four heat flux values are investigated, which are, 51, 76, 106, and 134 $kW.m^{-2}$, and the pressure is about 17 bar. Figure 5 illustrates the variation of heat transfer coefficient with the heat flux, for the four surface roughness values, mentioned above. It is obvious that, for the same heat flux, when the roughness increases, the heat transfer coefficient increases. That may be because; the higher roughness offers larger wet surfaces, and longer surface cavities, which surround the new originated bubble with a larger surface area, and that promotes for a faster forming of bubbles, and more heat transfer to the adjacent fluid. Moreover, these cavities promote for more turbulence intensity and better thermal mixing in the region where natural convection occurs.

These conditions may lead to a higher fluid bulk temperature, and accordingly, a smaller temperature difference between the surface and the fluid, which in turn, produces a higher heat transfer coefficient for the same heat flux. Figure 6 illustrates the variation of the heat transfer coefficient with the temperature difference. When the surface heat flux increases, the temperatures of all adjacent fluid particles; gas or liquid, will increase. This leads to a higher fluid bulk temperature, and accordingly, a lower temperature difference and a higher heat transfer coefficient. Figure 7 illustrates the percentages of increase in heat transfer coefficient values for the cases with 134 $kW.m^{-2}$ over those of the cases whose heat flux is 51 $kW.m^{-2}$, and for different surface roughness. The maximum percentage of increase in heat transfer coefficient is achieved with surface roughness of 1.4 μm. This may be because; the ability to transfer heat and to form, rapidly the smaller bubbles, increases with the increase in wet surface area, which occurs with larger roughness. These bubbles have a lower thermal conductivity and slower motion than those of the liquid, and accordingly, the heat transfer through these bubbles is more probable to decrease. Then increasing the roughness promotes for two factors that oppose each other, the first dominates with lower surface roughness, and helps increase the heat transfer coefficient with the increase of heat flux. The second one starts to be dominant when the roughness increases, and try to inhibit the effect of the first factor. These opposing effects drive the growing of percentage of increase in heat transfer coefficient when the roughness increases to the value of about 1.4 μm, and then, this percentage starts to decrease again. A correlation is suggested to fit the heat transfer coefficient, the roughness, the heat flux and the superheat temperature, which is;

$$h = 0.99\, Ra^{0.27}\, q^{0.93}\, \Delta T^{-0.87} \qquad (6)$$

The worst deviation of the measured values from those, which are calculated, using this correlation is about 6 %. Appendix (B) illustrates a comparison of some measured data with the corresponding calculated values using equation (6).

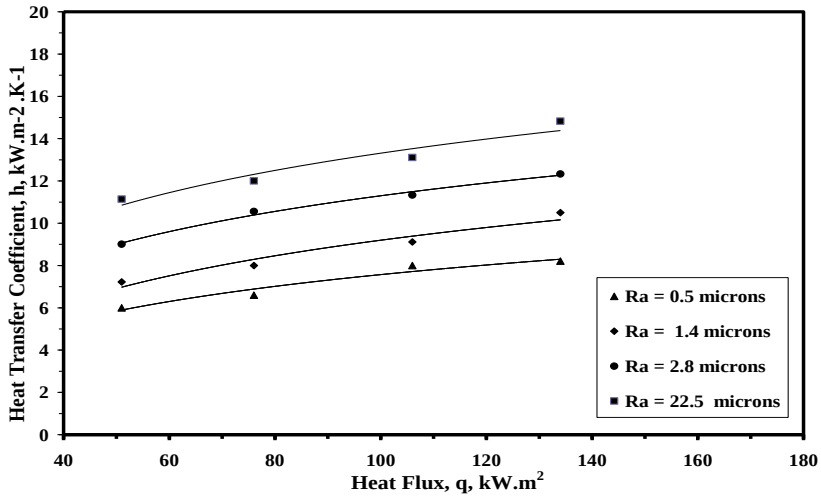

Figure 5: Variation of the heat transfer coefficient with the heat flux

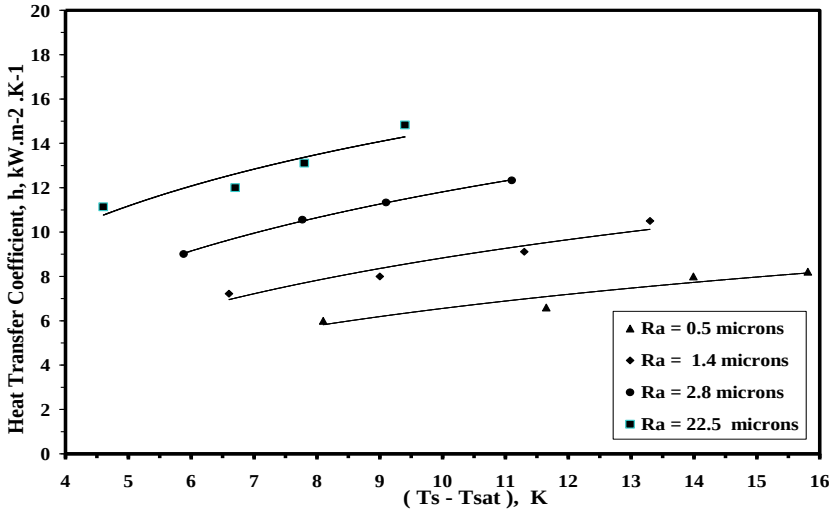

Figure 6: Variation of the heat transfer coefficient with the temperature difference

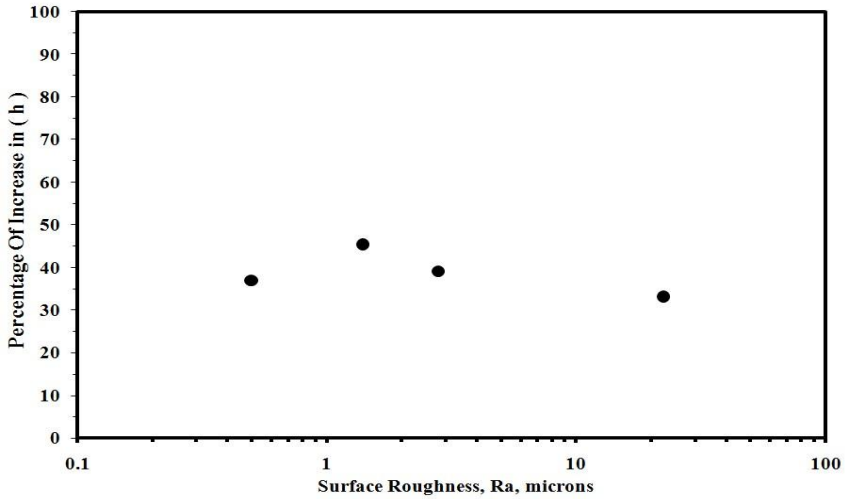

Figure 7: Variation of the percentage of increase in heat transfer coefficient with the surface roughness

4. Conclusion

In the present work, a controllable apparatus was implemented to investigate the heat transfer from a hot surface, to a refrigerant, R134a, in a pool boiling process. The surface roughness ranged from 0.5 to 22.5 μm and the heat flux, ranged from 51 to 134 $kW.m^{-2}$. The saturation pressure was about 17 bars. All conditions throughout the apparatus are controlled using Digital and PID control techniques. The experiments showed that, the heat transfer coefficient increased with the heat flux, for all values of surface roughness. For the same heat flux, the heat transfer coefficient increased with the surface roughness. The percentage of increase in the heat transfer coefficient at maximum heat flux over that at minimum heat flux occurred with surface roughness of 1.4 μm, and was about 47%. A correlation was suggested to fit the heat transfer coefficient, the roughness, the heat flux and the superheat temperature difference. The worst deviation of the calculated values using this correlation from the measured data was about 6%.

Acknowledgement

I ‘d like to thank prof. Mohammad Elfawal, head of the energy department, Nuclear and Radiological Regulatory Authority (NRRA), Egypt for his sincere help in producing the present work. Thanks also is attended to all technicians and supervisors of the heat transfer lab. In the faculty of engineering, Modern University, Egypt for their kind help.

References

[1]. Ryuichi Nagata,Chieko Kondou, and Shigeru Koyama, Comparative assessment of condensation and pool boiling heat transfer on horizontal plain single tubes for R1234ze(E), R1234ze(Z), and R1233zd(E), International Journal of Refrigeration, Volume 63, March 2016, Pages 157-170.

[2]. José Fernández-Seara, Ángel A. Pardiñas and Rubén Diz, Experimental heat transfer coefficients of pool boiling and spray evaporation of ammonia on a horizontal plain tube, International Journal of Refrigeration, Volume 67, July 2016, Pages 259-270.

[3]. José Fernández-Seara, Ángel Á. Pardiñas and Rubén Diz, Heat transfer enhancement of ammonia pool boiling with an integral-fin tube, International Journal of Refrigeration, Volume 69, September 2016, Pages 175-185.

[4]. Bartosz Zajaczkowski,Tomasz Halon and Zbigniew Krolicki, Experimental verification of heat transfer coefficient for nucleate boiling at sub-atmospheric pressure and small heat fluxes, Theyat Mass Transfer, (2016) 52:205–215, DOI 10.1007/s00231-015-1549-8.

[5]. Tong-Bou Chang and Zi-Long Wang, Experimental investigation into effects of ultrasonic vibration on pool boiling heat transfer performance of horizontal low-finned U-tube in TiO/R141b nanofluid, Theyat Mass Transfer, DOI 10.1007/s00231-015-1746-5, © Springer-Verlag Berlin Theyidelberg, 2016.

[6]. Marco Rossato, Davide Del Col, Angelo Muzzolon and Luisa Rossetto, Flow boiling of R32 inside a brazed plate heat exchanger, International Journal of Refrigeration, Volume 69, September 2016, Pages 165-174.

[7]. Evraam Gorgy and Steven Eckels, Convective boiling of R-134a on enhanced-tube bundles, International Journal of Refrigeration, Volume 68, August 2016, Pages 145-160

[8]. José Vicente Hallak d’Angelo,Vikrant Aute and Reinhard Radermacher Performance evaluation of a vapor injection refrigeration system using mixture refrigerant R290/R600a, International Journal of Refrigeration, Volume 65, May 2016, Pages 194-208.

[9]. O˘guz Emrah Turgut, Mustafa Asker and Mustafa Turhan Çoban, Saturated Flow Boiling Theyat Transfer Correlation for Small Channels Based on R134a Experimental Data, February 2016, King Fahd University of Petroleum & Minerals, Mechanical Engineering 2016.

[10]. V. Nikkhah and F. Hormozi, Pool boiling heat transfer of water/γ-alumina micro-fluids around the horizontal cylinder, Heat and Mass Transfer, April 2016, Volume 52, Issue 4, pp 763–772.

[11]. Mao-Yu Wen, Kuang-Jang Jang and Ching-Yen Ho, Boiling heat transfer and pressure drop of R-600a flowing in the mini-channels with fillisters, Theyat Mass Transfer (2015) 51:49–58DOI 10.1007/s00231-014-1394-1.
[12]. V. V. Kuznetsov and A. S. Shamirzaev, Boiling heat transfer of refrigerant R-21 in upward flow in plate-fin heat exchanger, Thermophysics and Aeromechanics, November 2015, Volume 22, Issue 6, pp 713–721.
[13]. M. M. Sarafraz, F. Hormozi and S. M. Peyghambarzadeh, E. Salari, Experimental study on the influence of SO_2 gas injection to pure liquids on pool boiling heat transfer coefficients, Heat and Mass Transfer, June 2014, Volume 50, Issue 6, pp 747–757.
[14]. M. E. Abo-Zeid, pool boiling heat transfer characteristics for R-134a on roughing surfaces, thesis, 2015, mechanical engineering department, Benha University, Egypt.
[15]. R. Hosseini, A. Gholaminejad and H. Jahandar, Roughness Effects on Nucleate Pool Boiling of R-113 on Horizontal Circular Copper Surfaces, World Academy of Science, Engineering and Technology 55 2011, pp 679-684.
[16]. S.W. Ahmad, T.G. Karayiannis, D.B.R. Kenning and Luke, Compound effect of EHD and surface roughness in pool boiling and CHF with R-123, Applied Thermal Engineering, Volume 31, Issues 11–12, August 2011, Pages 1994–2003.
[17]. José M. Saiz Jabardo, Gherhardt Ribatski and Elvio Stelute, Roughness, surface material effects on nucleate boiling heat transfer from cylindrical surfaces to refrigerants R-134a and R-123, Experimental Thermal and Fluid Science,Volume 33, Issue 4, April 2009, Pages 579–590.
[18]. Gherhardt Ribatski and José M.Saiz Jabardo, Experimental study of nucleate boiling of halocarbon refrigerants on cylindrical surfaces, International Journal of Theyat and Mass Transfer, Volume 46, Issue 23, November 2003, Pages 4439–4451.
[19]. S S. Bertsch, E A. Groll and S V. Garimella, Effects of Heat Flux, Mass Flux, Vapor Quality, and Saturation Temperature on Flow Boiling Heat Transfer in Microchannels, Purdue University Cooling Technologies Research Center, CTRC Research Publications, pp 1- 44, 2009.

APPENDIX A

Error Analysis

To estimate the uncertainties of the *derived* quantities, δA_s, δq and δh, we first recall the uncertainties of the *participating* quantities, which are;

The Length: is measured using a vernier caliper with uncertainty $\pm$ 0.02 mm

The Temperature: the MAX31855K output has 0.25 ^{o}C increment

The digital electrical measuring device has resolutions of 0.01 Volts and 0.01 Ampers

Then, we can estimate the uncertainties in the derived quantities as follows;

$$\delta A = (\frac{\pi d^2}{4})\sqrt{2(\frac{\delta d}{d})^2} \quad A.1$$

$$DQ = (98.3/100)\ x\ V\ x\ I\ \sqrt{(\frac{\delta V}{V})^2+(\frac{\delta I}{I})^2} \quad A.2$$

$$\delta T_{s,av} = \frac{\sqrt{4\delta T^2}}{4} = \frac{\delta T}{2} \quad A.3$$

$$\delta T_{r,av} = \frac{\sqrt{8\delta T^2}}{8} = \frac{\sqrt{2\delta T^2}}{4} \quad A.4$$

$$\delta h = \frac{Q}{A(T_{s,av}-T_{r,av})}\sqrt{(\frac{\delta Q}{Q})^2+(\frac{\delta A}{A})^2+\frac{\delta T_{s,av}{}^2+\delta T_{r,av}{}^2}{(T_{s,av}-T_{r,av})^2}} \quad A.5$$

Substituting the uncertainties in the participating quantities into eqn. A.5, we can estimate, the worst relative errors in the heat transfer coefficient, δh, which is 2.28 %.

APPENDIX B
CORRELATION TEST

Calculated Value Measured Value deviation

Calculated h, kW. $m^{-2}.T^{-1}$	**Experimental h, kW. $m^{-2}.T^{-1}$**	**Deviation**
8.50814	8.211	-3.61881
7.60362	8	4.9547
6.5357	6.6	0.974184
6.17616	6	-2.93603
10.1585	10.5	3.25227
9.40441	9.111	-3.2204
8.40195	8	-5.02443
7.58116	7.222	-4.9731
12.1042	12.33	1.83171
11.5581	11.333	-1.98616
9.72141	10.255	6.06
8.53575	9.011	5.27413
14.7772	14.8262	0.330743
13.89	13.10	-6.05
11.6837	12	2.63623
11.1623	11.1373	-0.224608